

## Electrophysiologic and Histologic Effects of Dissection of the Connections Between the Atrium and Posterior Part of the Atrioventricular Node

MARK A. MCGUIRE, MB, PhD, FRACP,\* MONICA ROBOTIN, MB, BS,  
ALEX S. B. YIP, MB, MRCP, JOHN P. BOURKE, MB, MRCP, DAVID C. JOHNSON, MB, FRACS,  
BARBARA I. DEWSNAP, PETER GRANT, MB, FRACS, JOHN B. UTHER, MD, FRACP,  
DAVID L. ROSS, MB, FRACP, FACC

Sydney, Australia

**Objectives.** This study was designed to examine the effects of destroying the posterior approaches to the atrioventricular (AV) node.

**Background.** Surgical and catheter ablation procedures have been developed for the cure of AV junctional reentrant tachycardia. Some of these destroy the posterior approaches to the AV node.

**Methods.** Atrioventricular node function and electrical excitation of Koch's triangle and the proximal coronary sinus were examined in 18 dogs. Dissection of the posterior atrionodal connections was performed in 10 dogs and a sham procedure in 8. After 28 to 35 days, repeat electrophysiologic and mapping studies were performed to assess changes in AV node function and the routes of AV and ventriculoatrial (VA) conduction. The AV junction was then examined with light microscopy.

**Results.** The compact AV node was undamaged in eight cases (80%). In two cases minor fibrosis occurred at the posterior limit of the compact node. The right-sided posterior atrionodal connections lying between the coronary sinus orifice and the tricuspid annulus were replaced by scar tissue in all cases, but the left-sided posterior connections and the anterior connections remained

intact. Atrioventricular and VA conduction intervals and refractory periods were not altered. Atrioventricular junctional echoes were present in 10 dogs before and in 7 dogs after dissection ( $p = 0.06$ ). Posterior (slow pathway) retrograde exits from the AV node were present in seven dogs before and in seven dogs after dissection. However, retrograde atrial excitation was altered in four of these seven dogs, so that the site of exit from the AV node was more leftward than it had been preoperatively. The node remained responsive to autonomic blocking drugs postoperatively. Double atrial electrograms similar to slow pathway potentials were found in all dogs.

**Conclusions.** This procedure ablates the posterior atrionodal connections but rarely damages the compact AV node. Atrioventricular node function is not impaired and the node is not denervated. The mechanism of cure of AV junctional reentrant tachycardia is probably damage to the perinodal atrium. This suggests that part of the slow AV node pathway may lie outside the compact AV node. Dual AV node exits and double atrial electrograms are present in the normal canine heart.

(*J Am Coll Cardiol* 1994;23:693-701)

Several effective surgical and catheter ablation procedures have been developed for the cure of atrioventricular (AV) junctional reentrant tachycardia (1-8). Some of these have been designed to destroy the posterior approaches to the AV node that lie between the coronary sinus orifice and the

tricuspid annulus (1,6-8). Lesions placed in this region frequently destroy or damage the slow pathway, which is thought to be the anterograde pathway in the anterior (typical) form of AV junctional reentrant tachycardia and the retrograde pathway in the posterior or atypical form of AV junctional reentrant tachycardia (1,6-8).

In 1983 we developed a surgical procedure for the cure of posterior AV junctional reentrant tachycardia (1). The latter is an atypical form of AV junctional reentrant tachycardia in which earliest retrograde atrial activation during tachycardia is found in the posterior part of Koch's triangle near the coronary sinus orifice (1,9,10). The surgical procedure was designed to interrupt the reentrant circuit at the point where the impulse emerged from the AV node and entered the atria. Thus, the aim was to section the posterior group of atrionodal connections, leaving the anterior atrionodal connections and the AV node intact. More recently it has been

From the Cardiology Department, Westmead Hospital, Sydney, New South Wales, Australia. This work was supported in part by a grant-in-aid from the Australian National Heart Foundation, Woden, Australian Capital Territory, Australia. Dr. McGuire is a recipient of a Postgraduate Medical Research Scholarship from the National Health and Medical Research Council, Woden. Dr. Bourke was supported by an Anglo-Australian Fellowship of the British Heart Foundation, London, England, United Kingdom.

Manuscript received April 19, 1993; revised manuscript received October 2, 1993, accepted October 25, 1993.

\*Current address: Cardiology Department, Royal Prince Alfred Hospital, Missenden Road, Camperdown, New South Wales, 2050, Australia.

Address for correspondence: Dr. David L. Ross, Cardiology Unit, Westmead Hospital, Westmead, New South Wales 2145, Australia.

demonstrated that the common or anterior type of AV junctional reentrant tachycardia can also be cured by the delivery of radiofrequency energy to the region posterior to the AV node (6-8).

Damage or destruction of the posterior atrionodal connections has a high success rate and low complication rate (1,6-8,11). However, it has not been possible to correlate the anatomic effects of this procedure with electrophysiologic changes because human tissue cannot be obtained for histologic examination. The aim of the current study was to examine the anatomic and electrophysiologic effects of damaging the posterior atrionodal connections in a canine model.

### Methods

The experimental protocol was approved by the Westmead Hospital Animal Research and Ethics Committee. The experimental animals were adult male or female mongrel dogs weighing 15 to 38 kg. Because it was necessary to examine the effects of the procedure on ventriculoatrial (VA) conduction, animals without demonstrable retrograde conduction were rejected from the study. In summary, AV and VA conduction were examined in 18 dogs using standard percutaneous techniques both in the baseline state and after the administration of autonomic blocking drugs. One week later, after institution of cardiopulmonary bypass, the electrical activation of Koch's triangle and the proximal coronary sinus was examined using a 60-electrode plaque. Surgical dissection of the posterior atrionodal connections was performed in 10 dogs and a sham procedure in 8 dogs. After 28 to 35 days, a second percutaneous electrophysiologic study was performed to assess changes in AV node function. One week later repeat mapping of electrical activation was performed during cardiopulmonary bypass to assess changes in the routes of AV and VA conduction. After fixation, the AV junction was cut in 5- $\mu$ m sections, and every 10th section was examined using light microscopy.

**Electrophysiologic studies.** Anesthesia was induced with sodium thiopentone (20 mg/kg, body weight intravenously). The dogs were then intubated and anesthesia was maintained with 0.5% to 1.5% halothane and a two to one mixture of nitrous oxide and oxygen. Three quadripolar 6F electrode catheters were then inserted into the right femoral vein using percutaneous techniques and advanced under fluoroscopic guidance to the high right atrium, the right ventricular apex and the AV junction in the region of the His bundle. Atrioventricular and VA conduction was examined using both the extrastimulus method and incremental pacing. Extrastimulus testing was performed using two drive cycle lengths set as close as possible to 350 ms and 300 ms. Single atrial extrastimuli were delivered after drive trains of 8 to 15 beats, and intervals of 3 s separated successive trains. The coupling interval of the initial extrastimulus was 10 ms less than the drive cycle length, and successive coupling intervals were shortened in 10-ms decrements until atrial refractoriness occurred. The coupling intervals of atrial

extrastimuli ( $A_1A_2$ ) were plotted against the AH interval ( $A_2H_2$ ) and the curve examined for the presence of discontinuities, which would suggest the presence of dual antero-grade AV node pathways. Incremental pacing was started at a cycle length 30 ms less than the sinus cycle length and then increased until second-degree AV block occurred.

Retrograde conduction was assessed in an analogous manner using ventricular stimulation. The coupling interval of ventricular extrastimuli ( $V_1V_2$ ) was plotted against the VA interval ( $V_2A_2$ ) and the curve examined for the presence of discontinuities, which would suggest the presence of dual retrograde AV node pathways. After completion of the stimulation protocol, atropine (0.4 mg/kg, 1 mg/min) and propranolol (0.2 mg/kg, 1 mg/min) were administered intravenously to induce blockade of the autonomic nervous system. The stimulation protocol was then repeated using drive cycle lengths as close as possible to those used in the baseline state. The purpose of inducing autonomic blockade was 1) to compare preoperative and postoperative AV node function without the confounding influence of autonomic tone, which might vary between the two studies, and 2) to allow assessment of the effects of the operative procedure on the autonomic innervation of the AV junction. The second (postoperative) electrophysiologic study was performed 4 to 5 weeks after the operative procedure, using a protocol identical to that used in the first study.

**Operative procedure.** After premedication with morphine (1 mg/kg) and atropine (0.04 mg/kg) administered subcutaneously, anesthesia was induced with sodium thiopentone (20 mg/kg) intravenously. The animal was intubated and anesthesia maintained with halothane 1.5% to 2.5% and a 2:1 nitrous oxide-oxygen mixture. Morphine (2 mg/kg) and pancuronium (0.04 mg/kg) were administered intravenously before dissection or the sham procedure was begun. A thoracotomy was performed in the right fifth intercostal space, and cannulas were placed in the left femoral artery and the superior and inferior venae cavae for cardiopulmonary bypass. On completion of mapping, a clamp was placed across the ascending aorta and a cardioplegic solution was infused into the aortic root. After arrest of the heart, either dissection of the posterior atrionodal connections or a sham procedure was performed. Detailed descriptions of these procedures are given later. The atriotomy was then closed and the aortic cross-clamp removed. The intercostal nerves in the region of the thoracotomy were infiltrated with 0.5% bupivacaine to provide postoperative analgesia, and supplementary morphine was administered subcutaneously as required.

The dissection technique has been previously described in detail (1,11,12). In summary, stay sutures were placed in the tricuspid annulus, and the right atrial endocardium was incised just above the tricuspid annulus. The endocardial incision extended from the central fibrous body to a point posterolateral to the coronary sinus orifice. The right atrial endocardium was then peeled back to expose the posterior septal space. The AV node, AV node artery, tendon of

Todaro and central fibrous body were identified. The posterior atrial connections of the AV node were then dissected from the node by dissecting the right ventricular free wall clean from the tricuspid annulus up to the posterolateral limits of the AV node. The inferior and anterior walls of the coronary sinus were then freed of atrial attachments from the mouth of the coronary sinus to close to the left atrial wall. This dissection was carried to the epicardium. The anterior approaches to the AV node were left intact. The endocardium was then repaired. In sham-operated animals the aortic cross clamp was applied and cardioplegic solution was infused, but no dissection was performed. The aortic cross clamp was removed after 15 min.

**Operative mapping.** Electrodes were fixed to the right ventricular outflow tract and the right atrial appendage for pacing. A 60-electrode mapping plaque was introduced through an oblique incision in the anterolateral wall of the right atrium. This plaque was similar to that described in detail in a previous report (13) except that the plaque used in the current study had a 2-mm rather than a 3-mm inter-electrode distance. Leads I, aVF and  $V_2$  were used to record the surface electrocardiogram (ECG). After positioning the plaque, the ventricles were paced slightly faster than the sinus rate and extrastimuli were delivered after drive trains of 8 beats. The first coupling interval was 40 ms less than the drive cycle length, and each successive coupling interval was decreased by 40 ms until ventricular refractoriness or failure of VA conduction. Intervals of 3 s separated successive trains. Methods of signal recording and processing have been described previously (13). Signals were recorded during sinus rhythm and ventricular pacing with a gain of 500 to 1,000 and bandpass of 0.2 to 500 Hz but an optional high pass analog filter (-3 dB point 35 Hz) was used for some recordings. Signals were digitized at 1,000 Hz with 12-bit accuracy and stored in the random access memory of a computer. The second mapping study was performed 28 to 36 days after the operative procedure. The anesthetic and mapping techniques were identical to those used at the first study except that the cardiopulmonary bypass oxygenator was primed with saline solution rather than heterologous blood.

**Histologic procedure.** At the completion of the second mapping study, sodium pentobarbitone (160 mg/kg) was administered intravenously. After cessation of cardiac activity, the heart was removed and fixed in 10% formalin. A block of tissue containing the AV junction in the region of the septum was excised. The anterior limit of the tissue block was the branching bundle, and the posterior limit was epicardium overlying the posterior septal space. The block was sectioned into slices of 5 mm and embedded in paraffin blocks. The plane of section was perpendicular to the plane of AV rings and perpendicular to the plane of the interatrial septum. Sections of 5- $\mu$ m thickness were cut, and every 10th section was stained with Gomori trichrome and examined with light microscopy.

**Statistical analysis.** Normally distributed data are expressed as mean value  $\pm$  SD, and the Student *t* test was used

for comparison. Non-normal group data were expressed as median and interquartile range (in parentheses), and differences between groups were examined using the Wilcoxon and Mann-Whitney tests. Commercially available software was used for analysis (StatView II, Abacus Concepts).

## Results

**Histologic examination.** In all cases the right-sided posterior approaches to the AV node were infiltrated by fibrous tissue, but the left-sided posterior approaches (those approaching from the left atrium along the course of the mitral annulus) were undamaged (Fig. 1 to 4). The compact AV node was undamaged in eight dogs, but minor fibrosis of the posterior limit of the compact node was present in two dogs (Fig. 5 and 6). The bulk of the compact node was undamaged in the latter two animals. In all animals scar tissue was present in the right atrial endocardium close to the anterior atrionodal connections, but the latter were intact (Fig. 6). This scar tissue appeared to have been caused either by the endocardial incision or by peeling back the endocardium to expose the posterior septal space. The His bundle was not damaged in any dog.

**Electrophysiologic studies. Sham procedure.** Before the operative procedure, the characteristics of anterograde conduction in the sham group were comparable to that of the dissection group whether assessed under basal conditions or under autonomic blockade. Preoperative characteristics of retrograde conduction in the sham group were similar to those of the dissection group except that the median VA relative refractory period was slightly longer in the sham group than in the dissection group. The sham procedure had no effect on AV or VA conduction either under basal conditions or under autonomic blockade.

**Anterograde AV conduction.** The dissection caused no significant change in anterograde conduction when measured under basal conditions or after autonomic blockade. Because the results were similar at both drive cycle lengths, they have been tabulated for one cycle length only (Tables 1 and 2). Postoperative anterograde conduction in the dissection group was similar to that in the sham group in the basal state and after autonomic blockade (results not tabulated). Before the operative procedure, discontinuities in the curve of  $A_1A_2$  versus  $A_2H_2$ , suggesting the presence of dual anterograde AV node pathways, were not present in any dog under basal conditions or after autonomic blockade. The AV node effective refractory period could not be measured in any dog because anterograde AV conduction was limited by refractoriness in the atrium rather than in the AV node.

**Retrograde conduction.** This was present in all dogs before and after dissection. Plots of  $V_1V_2$  versus  $V_2A_2$  did not reveal discontinuities suggestive of the presence of dual retrograde pathways in any animal. Dissection did not significantly affect any variable of retrograde conduction (Tables 1 and 2).

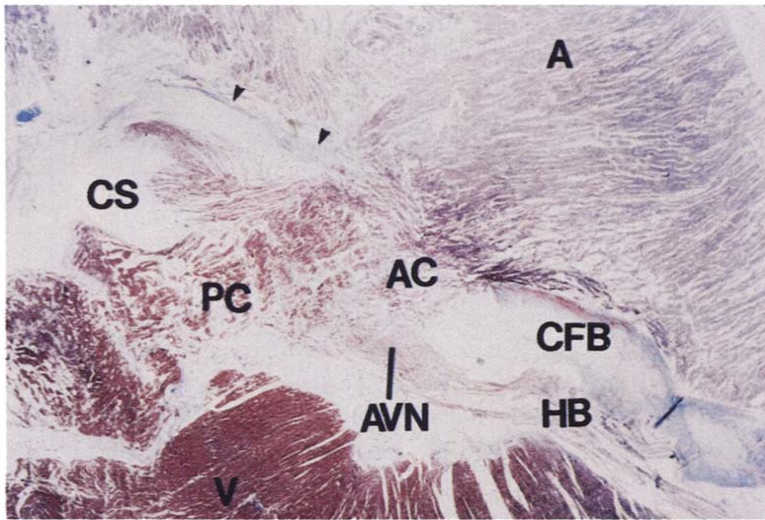


Figure 1. This section has been cut in a plane parallel to the cardiac septum. All sections have been stained with Gomori trichrome, which stains muscle fibers pink, red or mauve and fibrous tissue blue. The arrow heads indicate the tendon of Todaro. A = atrial myocardium; AC = anterior atrionodal connections; AVN = atrioventricular node; CFB = central fibrous body; CS = coronary sinus; HB = bundle of His; PC = posterior atrionodal connections; V = ventricular septum. Original magnification  $\times 6.7$ , reduced by 25%.

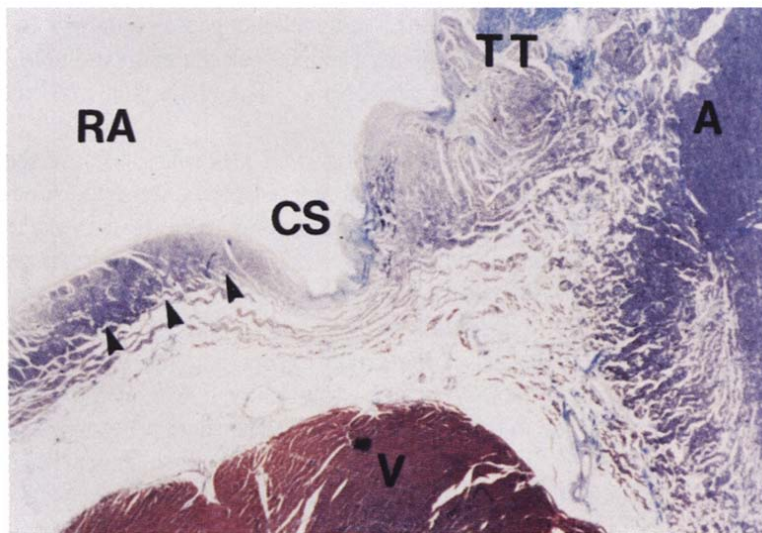


Figure 2. Section cut at the level of the anterior lip of the coronary sinus in a sham-operated dog. This section and subsequent sections have been cut in a plane perpendicular to the atrial septum and perpendicular to the tricuspid annulus. Note that the right-sided posterior approaches to the atrioventricular node (arrow heads) inferior to the coronary sinus orifice are intact. A = atrial septum; CS = coronary sinus orifice; RA = cavity of right atrium; TT = tendon of Todaro; V = ventricular septum. Original magnification  $\times 10$ , reduced by 25%.

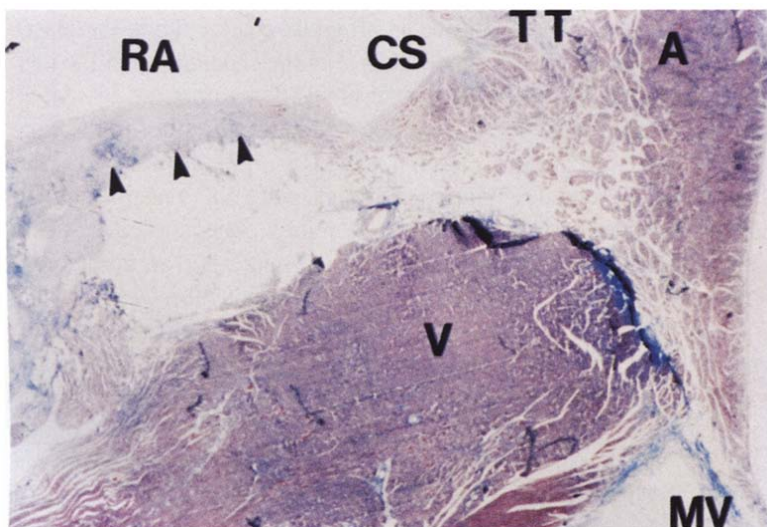
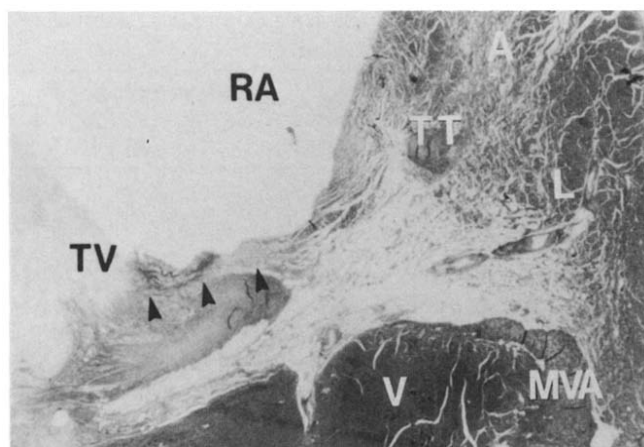


Figure 3. Section cut at the level of the anterior lip of the coronary sinus in a dog in which posterior atrionodal dissection has been performed. Note that the right-sided posterior approaches to the AV node (arrow heads) inferior to the coronary sinus orifice have been replaced by fibrous tissue (stained blue). MV = mitral valve; other abbreviations as in Figure 2. Original magnification  $\times 10$ , reduced by 25%.



**Figure 4.** Section from the level of the posterior atrionodal connections anterior to the coronary sinus in a dog in which posterior atrionodal dissection has been performed. Note that the right-sided posterior approaches to the atrioventricular node (arrow heads) are infiltrated by fibrous tissue, and dense fibrous tissue is present in the upper part of the tricuspid valve. The left-sided posterior approaches (L) to the atrioventricular node above the mitral valve annulus are intact and undamaged. MVA = mitral valve annulus; TV = tricuspid valve; other abbreviations as in Figure 2. Original magnification  $\times 10$ , reduced by 30%.

**AV junctional echoes.** These were not induced by atrial pacing in any dog. Before dissection, narrow complex AV junctional echoes were induced by ventricular pacing in 10 dogs (100%), but echoes could be induced in only 7 dogs after dissection ( $p = 0.06$ ).

**Autonomic blockade.** In dogs in which posterior dissection had been performed, the administration of autonomic blocking drugs at the postoperative electrophysiologic study caused significant impairment of AV and VA conduction, suggesting that the autonomic innervation of the AV node was intact (Table 3).

**Figure 5.** Section cut at the level of the posterior limit of the AV node in an animal in which posterior atrionodal dissection has been performed. Note that the posterior limit of the AV node is undamaged; other abbreviations as in Figures 2 and 4. Original magnification  $\times 10$ , reduced by 30%.

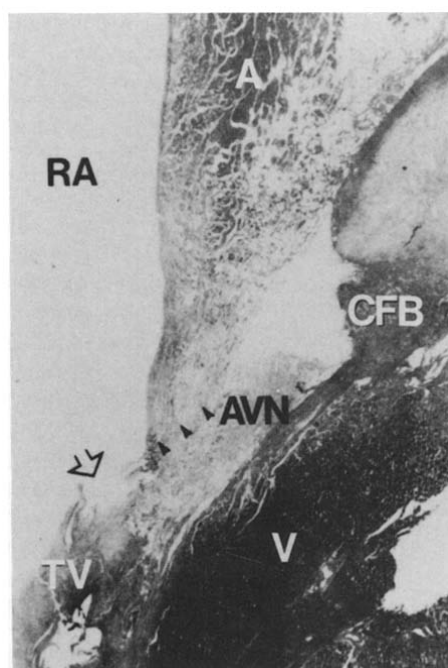
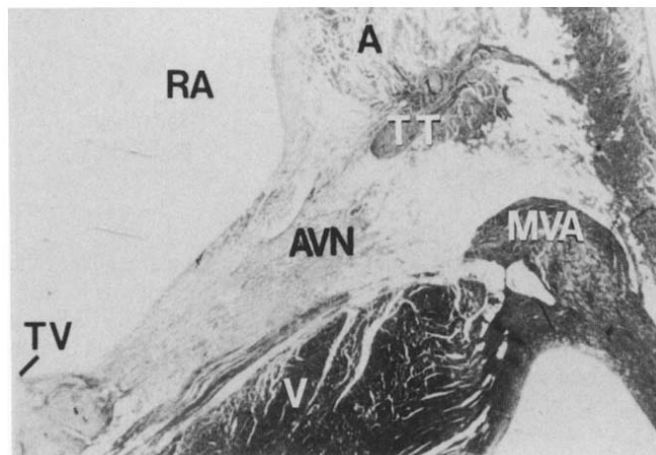


**Figure 6.** Section cut at the level of the anterior atrionodal connections in an animal in which posterior atrionodal dissection has been performed. Note that the compact AV node and anterior atrionodal connections (small solid arrow heads) are undamaged. The defect in the right atrial endocardium (large open arrow) just above the tricuspid annulus is a postmortem artifact caused by the removal of a suture before sectioning. Some scarring of the upper part of the septal leaflet of the tricuspid valve is evident. A = medial wall of right atrium; TV = septal leaflet of tricuspid valve; other abbreviations as in Figures 1 and 2. Original magnification  $\times 10$ , reduced by 30%.

**Double atrial potentials.** Atrial potentials with two or more components, similar to those reported in humans with AV junctional reentrant tachycardia, were observed in all dogs (6,8). The timing of the two components of the electrogram was not fixed, and small changes in the direction of the wave front of excitation (for example, sinus rhythm versus atrial pacing) caused small differences in the relative timing, suggesting that the two components arose from different muscle bundles (Fig. 7). Double electrograms were present in the region of the slow pathway exit but could be found at distances up to 1 cm from this exit. The double electrograms remained present postoperatively.

**Mapping of atrial activation.** Although plots of  $V_1V_2$  versus  $V_2A_2$  were smooth in all dogs, suggesting that dual retrograde AV node pathways were not present, the presence of inducible echoes suggested that dual pathways were, in fact, present. In six dogs dual AV node exits could be demonstrated during ventricular pacing at the preoperative mapping study (Fig. 8). In these dogs ventricular extrastimuli with long coupling intervals were conducted to the atria through a fast pathway that first excited the atrium close to the His bundle at the site of the anterior atrionodal connections. However, extrastimuli with short coupling intervals were conducted through a slower pathway that first

**Table 1. Effect of Dissection of Posterior Atrionodal Connections on Atrioventricular and Ventriculoatrial Conduction Variables Measured Under Basal Conditions**

	Preoperative (n = 10)	Postoperative (n = 10)	p Value
Sinus cycle length	<b>370</b> (344-472)	<b>386</b> (360-416)	0.61
PA	<b>29</b> (28-36)	<b>36</b> (32-36)	0.43
AH interval			
Sinus rhythm	<b>44</b> (40-48)	<b>44</b> (36-44)	0.55
At cycle length 300 ms	<b>50</b> (40-50)	<b>50</b> (50-60)	0.94
HV interval	<b>32</b> (28-32)	<b>32</b> (28-32)	0.56
Duration of QRS complex	<b>50</b> (44-52)	<b>50</b> (48-52)	0.16
AV Wenckebach cycle length	<b>175</b> (170-180)	<b>175</b> (160-190)	0.92
AVNRRP	<b>250</b> (230-260)	<b>245</b> (220-260)	0.92
AVNFRP	<b>215</b> (210-240)	<b>210</b> (200-220)	0.38
VA interval during drive cycle	<b>140</b> (130-150)	<b>130</b> (120-150)	0.32
VAERP	<b>225</b> (200-250)	<b>215</b> (190-260)	0.83
VARRP	<b>290</b> (280-310)	<b>295</b> (290-340)	0.24
VAFRP	<b>285</b> (250-310)	<b>295</b> (260-320)	0.72
VA Wenckebach cycle length	<b>270</b> (260-300)	<b>280</b> (260-310)	0.48

Values are expressed in milliseconds as median value (bold type) and interquartile range (in parentheses). Refractory periods were measured at a basic cycle length of 300 ms (anterograde) and as close as possible to 400 ms (retrograde). AV = atrioventricular; AVNFRP = AV node functional refractory period; AVNRRP = AV node relative refractory period; AV Wenckebach cycle length = longest cycle length of atrial pacing inducing second-degree AV block; PA = right atrial conduction time; VA = ventriculoatrial; VAERP = effective refractory period of the VA conducting system; VAFRP = functional refractory period of the VA conducting system; VARRP = relative refractory period of the VA conducting system.

excited the atrium near the orifice of the coronary sinus at the site of the posterior atrionodal connections (Fig. 1, 8 and 9). The VA intervals during slow pathway conduction were often only 10 to 30 ms longer than those during fast pathway conduction, an observation that explains why plots of V<sub>1</sub>V<sub>2</sub>

**Table 2. Effect of Dissection of Posterior Atrionodal Connections on AV and Ventriculoatrial Conduction Variables Measured After Autonomic Blockade**

	Preoperative (n = 10)	Postoperative (n = 10)	p Value
Sinus cycle length	<b>446</b> (408-460)	<b>444</b> (408-492)	0.58
PA	<b>34</b> (32-40)	<b>32</b> (20-36)	0.70
AH interval			
Sinus rhythm	<b>54</b> (44-56)	<b>54</b> (52-60)	0.11
At cycle length 300 ms	<b>60</b> (60-70)	<b>70</b> (60-80)	0.09
HV interval	<b>32</b> (28-32)	<b>32</b> (28-32)	0.32
Duration of QRS complex	<b>50</b> (44-56)	<b>50</b> (48-52)	0.31
AV Wenckebach cycle length	<b>215</b> (200-230)	<b>210</b> (210-240)	0.89
AVNRRP	<b>265</b> (250-280)	<b>270</b> (250-280)	0.95
AVNFRP	<b>250</b> (240-260)	<b>245</b> (230-260)	0.72
VA interval during drive cycle	<b>160</b> (150-180)	<b>180</b> (155-190)	0.33
VAERP	<b>300</b> (265-335)	<b>270</b> (230-315)	0.37
VARRP	<b>380</b> (380-380)	<b>380</b> (360-405)	0.94
VAFRP	<b>370</b> (320-380)	<b>320</b> (300-325)	0.39
VA Wenckebach cycle length	<b>360</b> (325-380)	<b>370</b> (325-400)	0.44

Values are expressed in milliseconds as median value (bold type) and interquartile range (in parentheses). Refractory periods were measured at a basic cycle length of 300 ms (anterograde) and as close as possible to 400 ms (retrograde). Abbreviations as in Table 1.

**Table 3. Effect of Autonomic Blocking Drugs After Dissection of the Posterior Atrionodal Connections**

	Basal (n = 10)	Autonomic Block (n = 10,* n = 7†)	p Value
Sinus cycle length	<b>386</b> (360-416)	<b>444</b> (408-492)*	0.008‡
PA	<b>36</b> (32-36)	<b>32</b> (20-36)*	0.06
AH interval			
Sinus rhythm	<b>44</b> (36-44)	<b>54</b> (52-60)*	0.005‡
At cycle length 300 ms	<b>50</b> (50-50)	<b>70</b> (60-80)*	0.005‡
HV interval	<b>32</b> (28-32)	<b>32</b> (28-32)*	0.32
Duration of QRS complex	<b>50</b> (48-52)	<b>50</b> (48-52)*	0.32
AV Wenckebach cycle length	<b>175</b> (160-190)	<b>210</b> (210-240)*	0.005‡
AVNRRP	<b>245</b> (220-260)	<b>270</b> (250-280)*	0.045‡
AVNFRP	<b>210</b> (200-220)	<b>245</b> (230-260)*	0.005‡
VA interval during drive cycle	<b>130</b> (120-150)	<b>180</b> (153-188)†	0.02‡
VAERP	<b>215</b> (190-260)	<b>270</b> (228-313)†	0.02‡
VARRP	<b>295</b> (290-340)	<b>380</b> (360-403)†	0.02‡
VAFRP	<b>295</b> (260-320)	<b>320</b> (300-375)†	0.03‡
VA Wenckebach cycle length	<b>280</b> (260-310)	<b>370</b> (325-398)†	0.008‡

\*, † = number of animals in each group; retrograde conduction was possible in only seven animals after autonomic blockade. ‡ = statistically significant result. Values are expressed in milliseconds as median value (bold type) and interquartile range (in parentheses). Abbreviations as in Table 1.

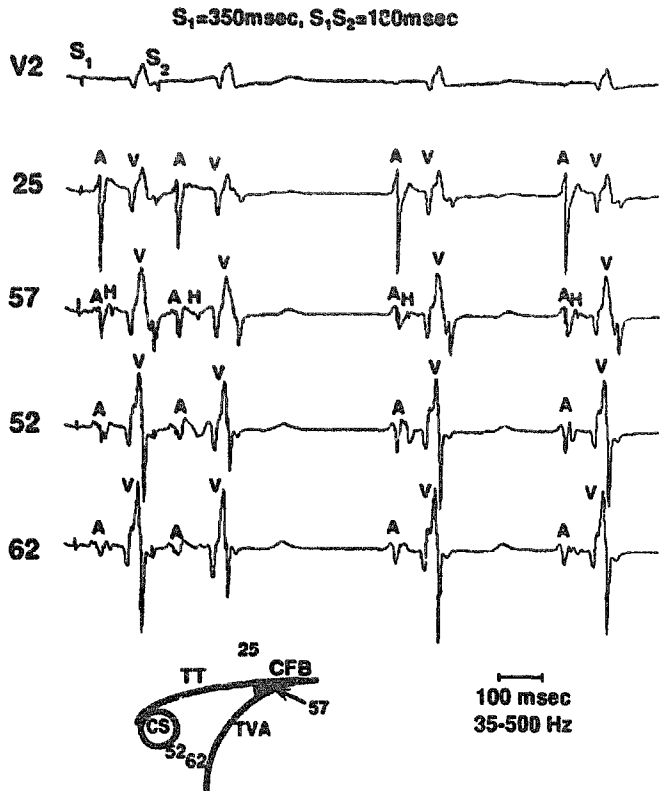


**Figure 7. Electrograms recorded from the perinodal region in the dog. Note the double potentials of the atrial electrograms in channels 52 and 62. The first beat is an atrial paced beat (S<sub>1</sub> = 350 ms) followed by an atrial extrasystole (S<sub>2</sub> = 180 ms) followed by two sinus beats. Upper channel is surface ECG lead V<sub>2</sub> (inverted). Positions of electrodes in other channels are shown at lower left. TVA = tricuspid valve annulus; other abbreviations as in Figures 1 and 2.**

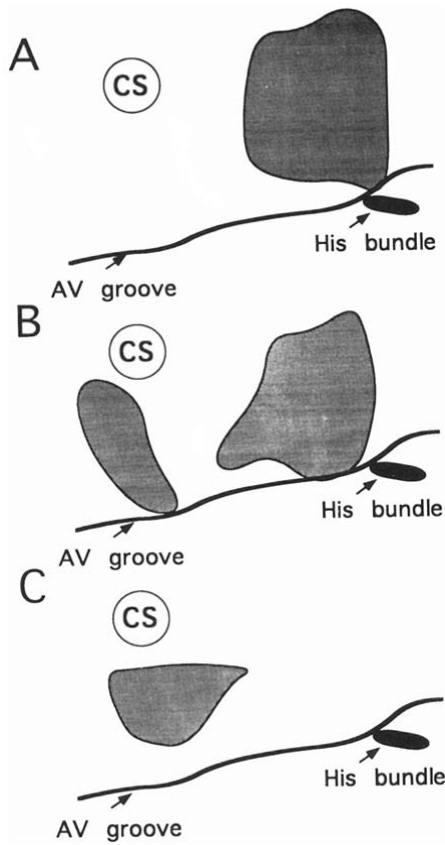


**Figure 8.** Sites of atrial exits from the AV node. The shaded regions show the areas enclosed by the first 3 ms of atrial excitation during ventricular pacing ( $S_1 = 320$  ms). **Panel A,** Excitation during a ventricular extrastimulus ( $S_2 = 280$  ms). The impulse is conducted through the anterior (fast pathway) exit. **Panel B,**  $S_2 = 240$  ms, conduction occurs simultaneously through both anterior and posterior exits. **Panel C,**  $S_2 = 200$  ms, the impulse blocks in the anterior pathway and is conducted through the posterior pathway, resulting in a ventricular echo with a narrow QRS complex.

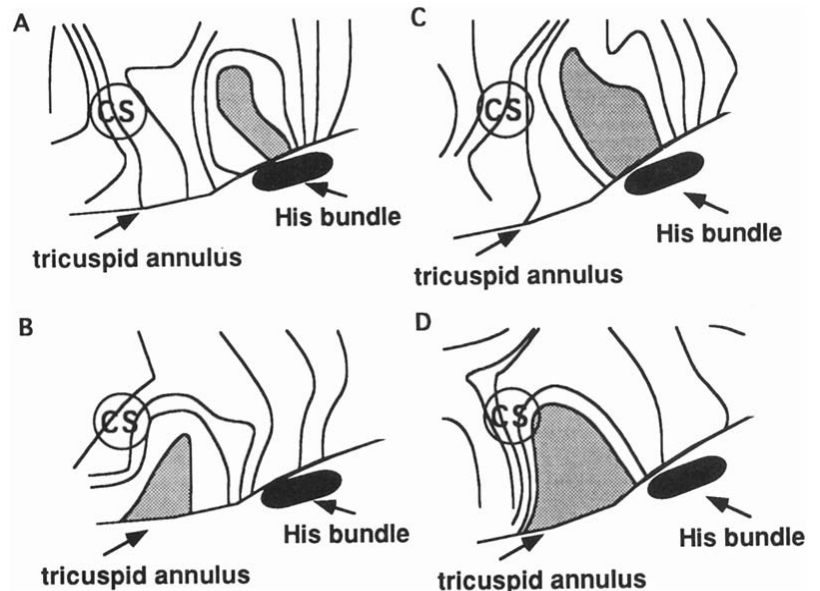
versus  $V_2A_2$  were smooth. Ventricular extrastimuli elicited a ventricular echo with a narrow QRS complex when the impulse was blocked in the fast pathway and was conducted through the slow pathway, attaining a critical delay in the VA interval. Only the fast pathway (anterior exit) was observed in three dogs, and only the slow pathway (posterior exit) was observed in one dog.

The postoperative mapping study demonstrated that the dissection did not destroy either the anterior or the posterior exits in any animal (Fig. 9). The pattern of retrograde atrial activation during *anterior* exit conduction was not altered. However, the pattern of atrial activation during *posterior* exit conduction was altered in four of seven dogs. In these dogs the site of earliest atrial activation before dissection was the endocardium of the right atrium between the coronary sinus orifice and the tricuspid annulus. However, after dissection, sites in the proximal coronary sinus were activated equally early, suggesting that the route of conduction through the posterior septal space was changed (Fig. 10). There was no significant difference, however, in the size of the area encircled by the isochrone marking the first 2 ms of atrial activation ( $11 \pm 9$  mm<sup>2</sup> vs.  $18 \pm 11$  mm<sup>2</sup>,  $p = 0.26$ , paired *t* test). The sham procedure did not alter the pattern of retrograde atrial activation in any animal.

### Discussion

The effects of dissection of the posterior atrionodal connections have not been studied extensively in humans with AV junctional reentrant tachycardia. Ross et al. (1) described three patients who had undergone posterior atrionodal dissection. That series was too small to determine the electrophysiologic effects of this procedure, but it is note-

**Figure 9.** Preoperative (A,B) and postoperative (C,D) maps of retrograde atrial excitation during ventricular pacing in a dog in which posterior atrionodal dissection had been performed. **Panels A and C** show drive cycle beats (cycle length 300 ms) that were conducted through the anterior atrionodal exit. **Panels B and D** show premature beats (coupling intervals 230 to 130 ms) that were conducted through the posterior atrionodal exit. Note that dissection did not destroy either exit. The patterns of preoperative and postoperative atrial activation during conduction through the posterior exit were similar in this dog. Isochrones were drawn at 2-ms intervals.



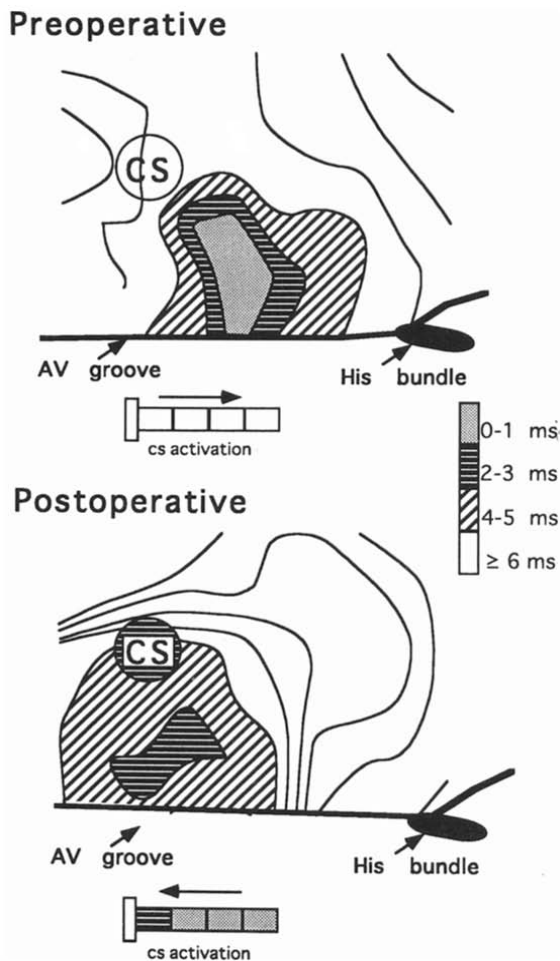


**Figure 10.** Change in pattern of retrograde atrial activation during conduction through the posterior atrionodal exit in a dog that had undergone dissection of the posterior atrionodal connections. Before dissection (top panel), earliest atrial activation was on the right atrial endocardial surface, and the coronary sinus (bar below each panel) was activated later, with activation spreading from the orifice toward the left. After posterior atrionodal dissection, the coronary sinus (CS) was activated in the reverse direction, and the coronary sinus was activated before the right atrial endocardium. AV = atrioventricular.

worthy that two of these patients had no demonstrable postoperative retrograde conduction. The current study indicates that this operative procedure does not directly damage the AV node in most cases. Moreover, AV node function is not altered, and the AV node remains responsive to autonomic blocking drugs. The pattern of retrograde atrial activation through the posterior atrionodal exit was altered in four of seven dogs, indicating that the normal route of exit from the AV node had been destroyed. These findings suggest that the mechanism of cure in humans with AV junctional reentrant tachycardia is damage to the putative atrial segment of the reentrant circuit located in the posterior approaches to the AV node between the coronary sinus orifice and the tricuspid annulus. This mechanism of cure is consistent with the finding that earliest atrial activation in humans with posterior AV junctional reentrant tachycardia

is in the same area (1,13). It is unlikely that autonomic denervation is responsible for cure because AV node conduction was unchanged in the baseline state and the AV node remained responsive to autonomic drugs after the procedure.

Although the pattern of retrograde atrial activation is altered in some cases, the posterior exits from the AV node are not completely ablated because posterior atrionodal connections remain on the left side of the septum. These connections contact the posterior aspect of the compact AV node through the left atrium near the mitral valve annulus. This finding explains why patients undergoing combined anterior and posterior dissection do not usually develop complete heart block (11). Clearly, in these patients these remaining left-sided posterior atrionodal connections provide the residual input to the AV node.

We (9) have previously presented evidence that three or more atrionodal connections exist in some patients with AV junctional reentrant tachycardia. We noted that the three groups of atrionodal connections described previously may represent the anatomic substrate of these connections. Because these three groups of connections are present both in humans with AV junctional reentrant tachycardia and in normal humans, it is likely that the abnormality causing the reentrant tachycardia is physiologic rather than anatomic. This thesis is consistent with the finding that the AV node appears structurally normal in patients with AV junctional reentrant tachycardia (14).

**Relation to radiofrequency ablation techniques.** Of interest is the recent discovery that anterior or common type of AV junctional reentrant tachycardia can be cured by the application of radiofrequency energy to a site similar to that damaged by the surgical method described in this report (6-8,15). This technique has been shown to destroy the slow AV node pathway, which is believed to represent the retrograde limb of the reentrant circuit in posterior AV junctional reentrant tachycardia and the anterograde limb of the circuit in anterior AV junctional reentrant tachycardia. The site of application of radiofrequency energy in the series of Jackman et al. (8) was in most cases between the coronary sinus orifice and the tricuspid annulus. This site is approximately  $17 \pm 3$  mm from the His bundle, and thus is approximately 10 mm from the posterior extent of the AV node because the AV node is  $<7$  mm long (16,17). This finding and the findings of the current study suggest that the slow AV node pathway or part of this pathway lies outside the compact AV node.

**Dual exits from the AV node of the normal dog heart.** The finding that dual AV node exits are present in normal dog hearts is surprising. As far as we are aware, this finding has not been demonstrated previously, although a similar phenomenon has been reported in humans with dual retrograde AV node pathways (18). Others (19,20) have demonstrated a "dual AV" transmission system and the echo phenomenon in dog hearts. They suggested that atrial tissue connected the upper ends of the pathways and that the conduction times of the two pathways might differ because of different routes of



conduction. They did not attempt to map the sites of exit from the AV node, but our findings in the current study suggest that these dual exits are the substrate of the dual transmission system. The presence of dual AV node exits in normal dog hearts suggests that these dual exits may be a universal phenomenon. However, they may not be demonstrable in all hearts because the two exits might have similar refractory periods, in which case conduction through the faster pathway would mask conduction through the slower pathway. If this assertion is correct, it is likely that the abnormality causing AV junctional reentrant tachycardia in humans is a functional rather than an anatomic problem.

**Double atrial electrograms.** Double atrial electrograms, similar to those found in our study, have been successfully used to target the delivery of radiofrequency energy to the site of the slow pathway (6,8). The fact that these electrograms may be found in the normal dog heart and in patients without AV junctional reentrant tachycardia (6) suggests that 1) the potentials are an epiphenomenon (i.e., they are not a reflection of slow pathway activation), or 2) slow pathways are present in all hearts but are not detected by current techniques. Our finding that these potentials may be present at sites remote from the site of earliest atrial activation during retrograde slow pathway conduction suggests that the first explanation is more likely.

**Limitations of this study.** Caution should be used in extrapolating our findings to the clinical situation. None of the dogs had demonstrable dual anterograde AV node pathways or inducible sustained AV junctional reentrant tachycardia. Nevertheless, the anatomy of the canine AV node is similar to that of the human AV node (16,21), and the dual AV node exits found in the current study are similar to those found in humans (1,13,18). Moreover, an anatomic study by Scheinman et al. (14) in a human with AV junctional reentrant tachycardia showed the AV node to be structurally normal, which suggests that the defect causing AV junctional reentrant tachycardia is physiologic rather than anatomic. For these reasons and because of the difficulties in performing anatomic studies in humans, we believe that our model was suitable for the purposes of the study. Similarly, we cannot be certain the double atrial electrograms found in the current study are identical to those described by Haissaguerre et al. (6) or Jackman et al. (8). Nevertheless, the potentials in the current study were found at sites similar to those they described.

**Conclusions.** This surgical procedure ablates the posterior atrionodal connections lying between the coronary sinus orifice and the tricuspid annulus but rarely damages the compact AV node. Atrioventricular node function is not impaired, and the AV node is not denervated by the procedure. The mechanism of cure of posterior AV junctional reentrant tachycardia is probably damage to the perinodal atrium. Dual exits from the AV node and double atrial electrograms are present in the normal dog heart.

---

We gratefully acknowledge the technical assistance of Erica Eves, Edward Freitas, Nurten Goktekin, Gabrielle Hancock, Leslie Hines, Anne Madden, Eve O'Connor, Damodar Pokhrel, Bill Sinai, Alan Steirn, Elisabeth Wallace, Ian Weir and the staff of the Animal Care Department, Westmead Hospital.

---

## References

1. Ross DL, Johnson DC, Denniss AR, Cooper MJ, Richards DA, Uther JB. Curative surgery for atrioventricular junctional ("AV nodal") reentrant tachycardia. *J Am Coll Cardiol* 1985;6:1383-92.
2. Cox JL, Holman WL, Cain ME. Cryosurgical treatment of atrioventricular node reentrant tachycardia. *Circulation* 1987;76:1329-36.
3. Fujimura O, Guiraudon GM, Yee R, Sharma AD, Klein GJ. Operative therapy of atrioventricular node reentry and results of an anatomically guided procedure. *Am J Cardiol* 1989;64:1327-32.
4. Lee MA, Morady F, Kadish A, et al. Catheter modification of the atrioventricular junction using radiofrequency energy for control of atrioventricular nodal reentry tachycardia. *Circulation* 1991;83:827-35.
5. Goy J-J, Fromer M, Schlaepfer J, Kappenberger L. Clinical efficacy of radiofrequency current in the treatment of patients with atrioventricular node reentrant tachycardia. *J Am Coll Cardiol* 1990;16:418-23.
6. Haissaguerre M, Gaita F, Fischer B, et al. Elimination of atrioventricular nodal reentrant tachycardia using discrete slow potentials to guide application of radiofrequency energy. *Circulation* 1992;85:2162-75.
7. Kay GN, Epstein AE, Dailey SM, Plumb VJ. Selective radiofrequency ablation of the slow pathway for the treatment of atrioventricular nodal reentrant tachycardia. *Circulation* 1992;85:1675-88.
8. Jackman WM, Beckman KJ, McClelland JH, et al. Treatment of supra-ventricular tachycardia due to atrioventricular nodal reentry by radiofrequency ablation of slow-pathway conduction. *N Engl J Med* 1992;327:313-8.
9. McGuire MA, Lau KC, Johnson DC, Richards DA, Uther JB, Ross DL. Patients with two types of atrioventricular junctional (AV nodal) reentrant tachycardia: evidence that a common pathway of nodal tissue is not present above the reentrant circuit. *Circulation* 1991;83:1232-46.
10. McGuire MA, Yip ASB, Lau KC, et al. Posterior ("atypical") atrioventricular junctional reentrant tachycardia. *Am J Cardiol*. In press.
11. Johnson DC, Nunn GR, Meldrum-Hanna W. Surgery for atrioventricular node reentry tachycardia: the surgical dissection technique. *Semin Thorac Cardiovasc Surg* 1989;1:53-7.
12. McGuire MA, Ross D, Johnson D. Surgical techniques for the cure of atrioventricular junctional reentrant tachycardia. *Coronary Art Dis* 1992; 3:186-91.
13. McGuire MA, Bourke JP, Robotin MC, et al. High resolution mapping of Koch's triangle using sixty electrodes in humans with atrioventricular junctional ("AV nodal") reentrant tachycardia. *Circulation* 1993;88(part 1):2315-28.
14. Scheinman MM, Gonzalez R, Thomas A, Ullot D, Bharati S, Lev M. Reentry confined to the atrioventricular node: electrophysiologic and anatomic findings. *Am J Cardiol* 1982;49:1814-8.
15. Jazayeri MR, Hempe SL, Sra JS, et al. Selective transcatheter ablation of the fast and slow pathways using radiofrequency energy in patients with atrioventricular nodal reentrant tachycardia. *Circulation* 1992;85:1318-28.
16. Widran J, Lev M. The dissection of the atrioventricular node, bundle and bundle branches in the human heart. *Circulation* 1951;4:863-7.
17. McGuire MA, Johnson DC, Robotin MC, Uther JB, Ross DL. Dimensions of the triangle of Koch in humans. *Am J Cardiol* 1992;70:829-30.
18. Sung RJ, Waxman HL, Saksena S, Juma Z. Sequence of retrograde atrial activation in patients with dual atrioventricular nodal pathways. *Circulation* 1981;64:1059-67.
19. Moe GK, Preston JB, Burlington H. Physiologic evidence for a dual A-V transmission system. *Circ Res* 1956;4:357-75.
20. Mendez C, Han J, Garcia de Jalón PD, Moe GK. Some characteristics of ventricular echoes. *Circ Res* 1965;16:562-81.
21. Racker DK. Atrioventricular node and input pathways: a correlated gross anatomical and histological study of the canine atrioventricular junctional region. *Anat Rec* 1989;224:336-54.